Applied Thermal Engineering 180 (2020) 115788

Contents lists available at ScienceDirect

Applied Thermal Engineering

journal homepage: www.elsevier.com/locate/apthermeng

Experimental investigation and cost analysis on a nanofluid-based desalination system integrated with an automatic dual-axis sun tracker and Fresnel lens

Sina Abbaszadeh Hashemi[a], Mohsen Kazemi[a], Amin Taheri[a], Mohammad Passandideh-Fard[a,*], Mohammad Sardarabadi[b,*]

[a] Department of Mechanical Engineering, Ferdowsi University of Mashhad, Mashhad, Iran
[b] Department of Energy, Quchan University of Technology, Quchan, Iran

HIGHLIGHTS

- Performance of the CSS integrated with a two-axis STS and Fresnel lens was investigated.
- Effect of MWCNT/water nanofluid on improvement of fresh-water productivity was studied.
- Cost, energy and fresh-water productivity analysis on four various setups were performed.
- Total yield of fresh-water of CSS with STS was enhanced by 6100 mL/(m^2·day) compared to that of CSS.
- Utilizing nanofluid and STS, the cost of fresh-water productivity was reduced by 0.206 $/liter.

GRAPHICAL ABSTRACT

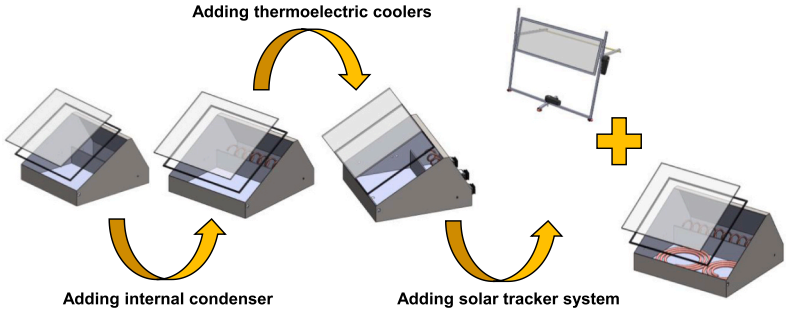

ARTICLE INFO

Keywords:
Desalination system
Fresnel lens
Multiwall carbon nanotubes (MWCNTs)
Solar still
Solar tracking system (STS)

ABSTRACT

In this experimental work, the performance of a nanofluid-based solar still equipped with a dual-axis solar tracker system (STS) has been investigated through various viewpoints, i.e., daily and nightly fresh-water production, hourly and daily efficiency and cost. The proposed solar still consists of a conventional solar still (CSS), three Fresnel lens concentrator, and an active automatic STS. Moreover, the effects of deionized water, MWCNTs/water nanofluid with two mass fractions of 0.15 and 0.3%, as the heat transfer fluid (HTF), are studied on fresh-water productivity to evaluate the appropriate HTF type. The daily, nightly, and total fresh-water produced by the CSS with internal condenser is found to be 2180, 560, and 2740 mL/(m^2·day), respectively. However, the CSS integrated with STS and Fresnel lens can produce daily, nightly, and total fresh-water of 5310, 1080, and 6390 mL/(m^2·day), respectively. In addition, the results indicate that using MWCNTs/water nanofluid with a mass fraction of 0.3% enhances fresh-water productivity by 31.6, 7.4, and 27.5%, respectively, compared to that of pure water as HTF. The results reveal that by using the nanofluid with a mass fraction of 0.15 and 0.3%, the daily average efficiency is increased about 9.56 and 17.85%, respectively, compared to that of pure water as HTF.

* Corresponding authors.
E-mail addresses: mpfard@um.ac.ir (M. Passandideh-Fard), m.sardarabadi@yahoo.com (M. Sardarabadi).

https://doi.org/10.1016/j.applthermaleng.2020.115788
Received 29 December 2019; Received in revised form 27 May 2020; Accepted 21 July 2020
Available online 25 July 2020
1359-4311/

1. Introduction

The fresh-water is a vital substance for the existence of life on earth. However, the amount of clean, drinkable, and accessible water is reducing rapidly because of an increase in water pollution and a swelling population. 97% of the water in the globe is in the lakes, seas, and oceans, and only about 3% is available as fresh water and 1% as drinkable [1]. Oceans are the infinite sources of saline water. Desalination is a promising and suitable solution to eliminate salt to produce drinkable water. However, removing salts from seawater needs large amounts of energy usually supplied by burning fossil fuels which in turn leaves irrecoverable impacts on the environment and human health. Thus, improving the efficiency of desalination systems and utilizing renewable energies can be effective ways to decrease the environmental damages.

Desalination systems can be divided into two main groups: large scale or commercial and small scale or domestic. There are different technologies and processes for desalination in large scales, like multi-stage flash, multi-effect, membrane, reverse osmosis and distillation [2–5]. These types of desalination systems are energy-consuming; replacing these methods with alternative ways that are eco-friendly and affordable like solar and wind energies are preferred. Small-scale desalination systems mostly use solar energy as an alternative and inexpensive energy [6]. In domestic desalination systems, although the fresh-water production of solar stills is low, they are sustainable and affordable. Desalination by solar energy continues to attract a lot of research interest targeted to enhance their fresh-water productivity. Two main keys for solar desalination are evaporation and condensation. Solar energy evaporates the brine water and the condenser collects the distilled water [7]. There are several experimental and theoretical research available in the literature carried out to increase solar stills productivities [8–11]. Based on energy consumption, solar stills are categorized into two main types: passive and active [12]. Passive solar stills carry out the desalination process without any external source [6]. Low fresh-water yield is the main weakness of passive solar stills which is in the range of 3–6 kg/(m^2·day) [13]. To tackle the problem of passive solar stills, some external sources such as concentrator, collector, or indirectly heat exchanger are utilized to increase the feed-water temperature in the basin. These hybrid systems are introduced as the active solar stills [14]. Some items play important roles in the efficiency of solar desalination like feed-water temperature, water depth [15], glass cover angle, material used, and surface area [15,16].

Water temperature is mostly used as the base for categorizing active solar stills such as flat plate solar collectors [17,18], parabolic solar collectors [19,20], photovoltaic thermal systems [9,21,22], heat pipes [23,24], Fresnel collectors [18,25], and Fresnel concentrators [26–30]. In these systems, preheating of water is used to increase the fresh-water productivity. A major drawback of these active solar stills is their inability to receive maximum solar radiation during the daylight. Integrating a solar tracker system (STS) with these solar stills can eliminate their weakness.

A STS follows the sun position and receives the maximum solar irradiation. The STSs based on their tracking system are divided into two main categories: one-axis and two-axis. The performance of solar absorption in a two-axis STS is enhanced compared to that of one-axis STS and fixed systems. This is because the sunlight is perpendicular to the surface at each time and harvesting more solar irradiation in a two-axis compared to that of a one-axis in which the surface is fixed. Based on the literature, using the STS with a Fresnel lens concentrator for heating the feed-water is rare. Very recently, a modified nanofluid-based active solar distillation system has been proposed by Muraleedharan et al. [31]. Their system consists of the CSS, one-axis STS, and linear Fresnel lenses linked to an evacuated receiver tube with a serpentine heat exchanger. They found that the hourly fresh-water production of modified solar distillation system using Al_2O_3/water nanofluid with a volume fraction of 0.1%, as the working fluid, can be increased up to 250% compared to the CSS. The total fresh-water produced by the modified solar distillation system (0.1% nanofluid) and the CSS was 12.190 L/(m^2·day) and 3.48 L/(m^2·day), respectively.

According to the aforementioned literature review, many schemes and designs have been proposed and investigated by researchers to enhance the fresh-water production of the CSS. However, less efforts have been made to enhance the efficiency of the CSS with the aid of solar tracking systems. Additionally, the literature shows that the nanofluids, as working fluids, have a crucial role in improving fresh-water production. Consequently, in the current experimental study, an active nanofluid-based solar still system is investigated. This solar still consists of linear Fresnel lenses based on a concentrator linked to a dual-axis robotic sun tracker which is connected to the CSS with two slopes. The feed-water in the CSS is heated by a spiral heat exchanger where heat transfer fluid (HTF) absorbs solar energy from STS which is equipped with Fresnel lenses. The main purpose of this study is on increasing the efficiency of fresh-water production with the aid of STS. In addition, the effect of deionized water, MWCNTs/water with two weight fractions of 0.15 and 0.3%, as the HTFs, are investigated. The results of proposed active solar still are compared to those of the CSS with an internal condenser and also the CSS equipped with both an internal condenser and external thermoelectric coolers. The results of the present study can be used to improve future solar stills design and help scholars who work on renewable energies.

2. Experimental apparatus and nanofluid preparation

2.1. Experimental setup description

As mentioned before, in this study, four different setups are investigated (named A, B, C, and D):

- Setup A: The first system is a conventional system (setup A in Fig. 1); the structure is made from galvanized steel with a thickness of 1.25 mm and a two-slope solar still which is considered to increase the condensation. The north side of the CSS is made from galvanized steel and the south side from the glass with 6 mm thickness installed with an angel of 30° with respect to the horizontal surface. In order to decrease the heat losses, the outside part of the solar still is covered with two insulation layers with a thickness of 10 mm.
- Setup B: The second setup is similar to the setup A, but in order to increase the condensation rate, this system is equipped with a helical copper coil whose length, inner diameter, and outer diameter are 9 m, 6 mm, and 8 mm, respectively (setup B in Fig. 1). The cold water enters the helically coiled condenser with a temperature of 20 °C.
- Setup C: This setup is the same as setup B except that three external thermoelectric coolers are added to the system (setup C in Fig. 1).
- Setup D: In the fourth system, the CSS is connected to a dual-axis STS with three linear Fresnel lenses to increase the feed-water temperature by a spiral copper heat exchanger which is placed in the CSS. The proposed STS follows the sun with the aid of four sensors and two DC electro-motor linked to a controller circuit. It should be noted that the HTFs (deionized water and two mass fractions of MWCNTs/water nanofluid) pass through spiral-shaped coils are placing at the bottom of the CSS (setup D in Fig. 1).

In this study, the absorber pipe for the collector is made of copper with a suitable thermal conductivity/flexibility and high-pressure durability. Moreover, the copper tube is used for the heat exchanger in the CSS with the purpose of increasing the evaporation rate. Two copper tubes which are spiral-shaped are placed at the bottom of the solar still (see setup D). The outer and inner diameters of the copper tube in the collector and heat exchanger are 12 and 10 mm, respectively. The length and focal length of the linear Fresnel lens are 960 and 600 mm, respectively, and the surface area exposed to the incident solar

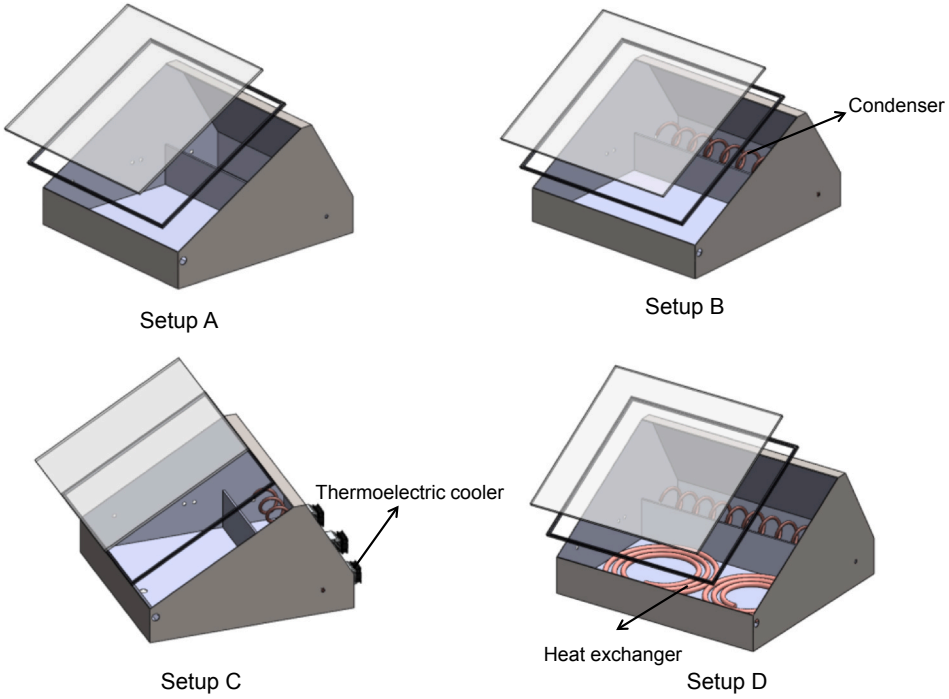

Fig. 1. A 3D schematic of all studied setups.

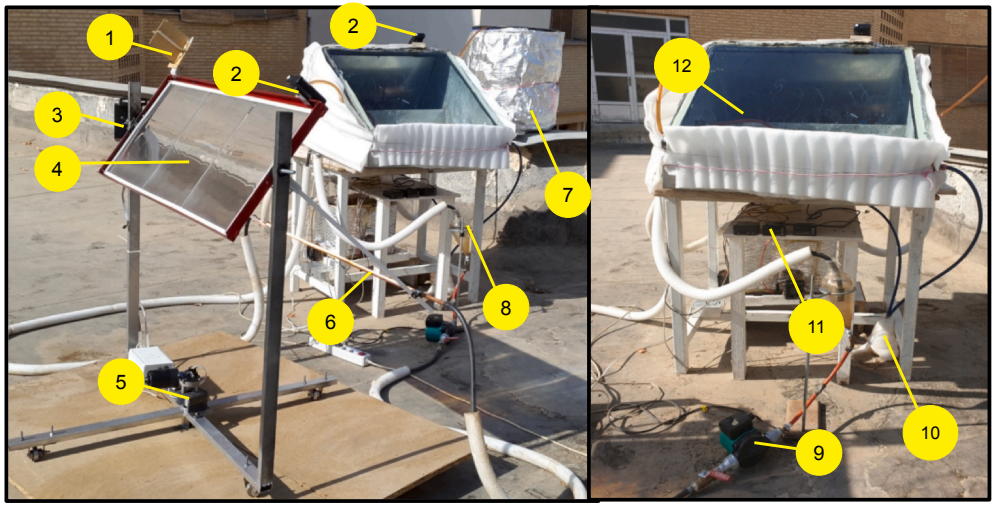

Fig. 2. Actual image of the experimental setup.

irradiation is 0.384 m^2. To track the sun location throughout the daylight, a dual-axis STS is designed. One centrifugal pump is used to circulate the HTF between the collector and heat exchanger in a closed loop. The outdoor experiments are conducted on sunny and stable days in June 2019 at the Ferdowsi University of Mashhad, Iran (36.26°N, 59.61°E). An actual image and schematic illustration of the experimental setups are shown in Figs. 2 and 3, respectively.

The following instruments are utilized for manually recording various parameters in this experimental study:

- The intensity of solar irradiation at the inclined south side of STS and the CSS is recorded manually using two same solar power meters, TES-1333 (number 2 in Fig. 2).
- The HTF temperature in both inlet and outlet of the heat exchanger and collector and feed-water temperature in the CSS are measured with PT-100 thermocouples.
- Two measuring cylinders with a precision of 10 mL is used to collect and measure produced fresh-water. Measuring instruments and their related sections in the experiments are summarized in Table 1.

2.2. Preparation and characterization of MWCNTs/water nanofluid

The MWCNTs nanoparticles and deionized water, whose specifications are summarized in Table 2, are used in the current experimental study. The use of MWCNTs/water nanofluid is because of its better thermal properties and stability with respect to the other nanofluids.

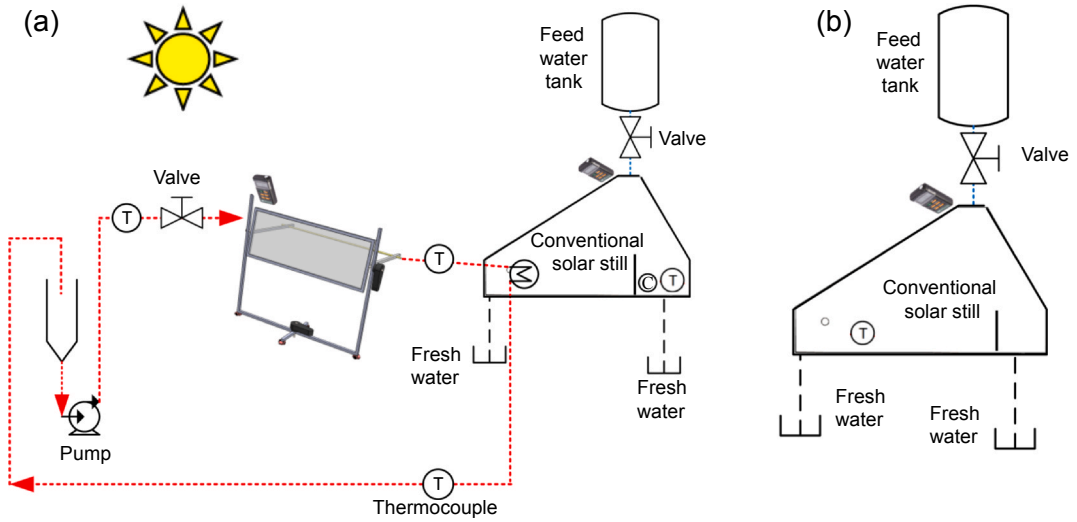

Fig. 3. Schematic diagram of (a) setup D (b) setup A.

Table 1
Measuring instruments and their related sections in the experiments.

Inlet and outlet HTF temperatures	RTD-PT100 thermocouple
Feed-water temperature	RTD-PT100 thermocouple
Inlet and outlet working fluid temperatures	RTD-PT100 thermocouple
Ambient temperature	Mercury thermometer
Solar irradiation	Pyranometer-TES133

Table 2
Nanoparticles and base-fluid properties [32].

Material	ρ (kg/m^3)	k (W/m·K)	C_p (J/kg·K)
MWCNTs-OH nanoparticles	1600	3000	796
Water	997.0	0.613	4179

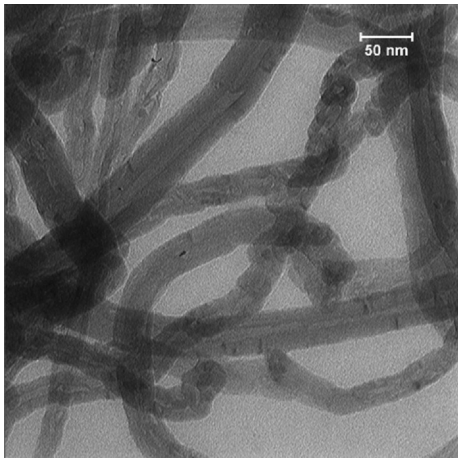

Fig. 4. The TEM image of MWCNTs nanoparticles.

The MWCNTs nanoparticles are purchased in the dry form with a purity of +95% from VCN Nanomaterials Company in Iran. The TEM image of the MWCNT nanoparticles is illustrated in Fig. 4. The regular length, diameter, and specific surface area of studied nanoparticles are 5–10 μm, 20–30 nm, and +200 m^2/g, respectively. The MWCNTs nanoparticles with the proper mass fractions are dispersed into deionized water using high-speed stirring (for 1 hr.) followed by ultrasonic vibration (4 cycles-30 min period).

3. Error analysis and uncertainty

The experiments are conducted after calibrating all measuring instruments including PT-100 thermocouples, light sensors, solar meters, and mercury thermometer. Generally, in the experimental studies, the uncertainty analysis is performed with various methods to ensure the reliability of the obtained data. In this study, the uncertainty calculations are carried out based on the methodology presented elsewhere [33,34]. The maximum uncertainty of the data and accuracy of measuring instruments are reported in Table 3.

4. Results and discussion

In this experimental study, four different setups including the CSS (setup A), the CSS with an internal condenser (setup B), the CSS with an internal condenser and external thermoelectric coolers (setup C), and the CSS with an internal condenser and external thermoelectric linked to a solar tracker system (setup D) are investigated. Furthermore, the effects of deionized water and two mass fractions of MWCNTs/water nanofluid (0.15 and 0.3%) are studied on the performance of the setup D. In the following sections, the results of four different setups are compared to each other in terms of fresh-water production, feed-water temperature, average daily efficiency, and cost analysis.

Table 3
Uncertainties of the measuring instruments.

Instruments	Model	Measurement section	Accuracy	Maximum uncertainty
Solar meter	TES-133	Solar irradiation	± 10 W/m^2 + 0.38 W/m^2 for (T_{ref} + 1)	5.6 W/m^2
Thermocouple	PT-100	Feed-water temperature	± 0.15–0.25 °C	0.17 °C
Thermocouple	PT-100	Working fluid temperature	± 0.15–0.25 °C	0.14 °C
Thermocouple	PT-100	HTF temperature	± 0.15–0.25 °C	0.12 °C
Thermometer	Mercury	Ambient temperature	+0.5 °C	0.4 °C

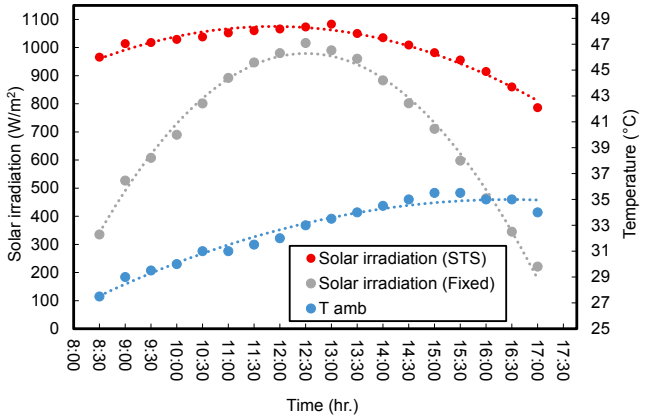

Fig. 5. Variation of ambient temperature and solar irradiation versus local time.

4.1. Operation conditions

The variation of operating conditions including the solar irradiation on the CSS, the solar irradiation on the STS (maximum received solar irradiation), and the ambient temperature from 8:30 to 17:00 in the month of July at this location (Latitude: 36.2˚ and Longitude: 59.1˚) during the experiments is displayed in Fig. 5. According to this figure, the maximum, minimum, and average of solar irradiation on the STS are nearly 1083 W/m^2, 776 W/m^2, and 999 W/m^2, respectively. The corresponding values for solar irradiation on fixed the CSS are 1016 W/m^2, 221 W/m^2, and 709 W/m^2, respectively. It is clear that the solar irradiation values for dual-axis STS are higher than those of the fixed system because of the change of the sun position in the sky. In addition, the average ambient temperature measured by a thermometer is 32.83 ˚C. As a result of the small differences in the inclination angle between the CSS and STS at the noon time, the maximum values of solar irradiations for the two systems are slightly different. In fact, to have a maximum solar radiation during a day in summer at the location of the experiment (Latitude: 36.2˚ and Longitude: 59.1˚), the CSS angle was fixed at 30˚ facing towards the south. The STS, however, continuously follows the sun's position. Right at the noon time the angle of the STS was about 35˚. Note that, the values of outdoor operating conditions including ambient temperature and solar irradiation depend on the time and location of the experiments.

4.2. Selection of mass flow rates for Fresnel lens (HTF) and condenser (working fluid)

In this research, for the purpose of determining the appropriate flow rates of condenser working fluid and HTF, a series of experiments are performed on setups B and D, respectively. First, the variation of daily total fresh-water accumulation versus local time for the setup B for the condenser working flow rates of 30 L/hr, 50 L/hr, and 70 L/hr is shown in Fig. 6(a). It is evident from this figure that by increasing the flow rate of the condenser from 30 L/hr to 50 L/hr, the total water accumulation is enhanced by 32.9%. While this value for increasing the flow rate from 50 L/hr to 70 L/hr is just 10.5%. Therefore, based on a remarkable increase of fresh-water production for a flow rate of 50 L/hr, this flow rate is selected for the condenser working fluid for the rest of the experiments in this study. Next, for a fixed condenser flow rate of 50 L/hr, by varying the HTF flow rate from 10 L/hr to 30 L/hr, the daily total fresh-water accumulation with respect to the local time for setup D is illustrated in Fig. 6(b). Based on this figure, the total water accumulation for 10 L/hr, 20 L/hr and 30 L/hr are 5310 mL/(m^2·day), 4190 mL/(m^2·day), and 3700 mL/(m^2·day), respectively. In fact, decreasing the HTF flow rate leads to an increase in feed-water temperature and improving the evaporation rate. Consequently, the 10 L/hr is selected for the HTF flow rate for the rest of the experiments in this study.

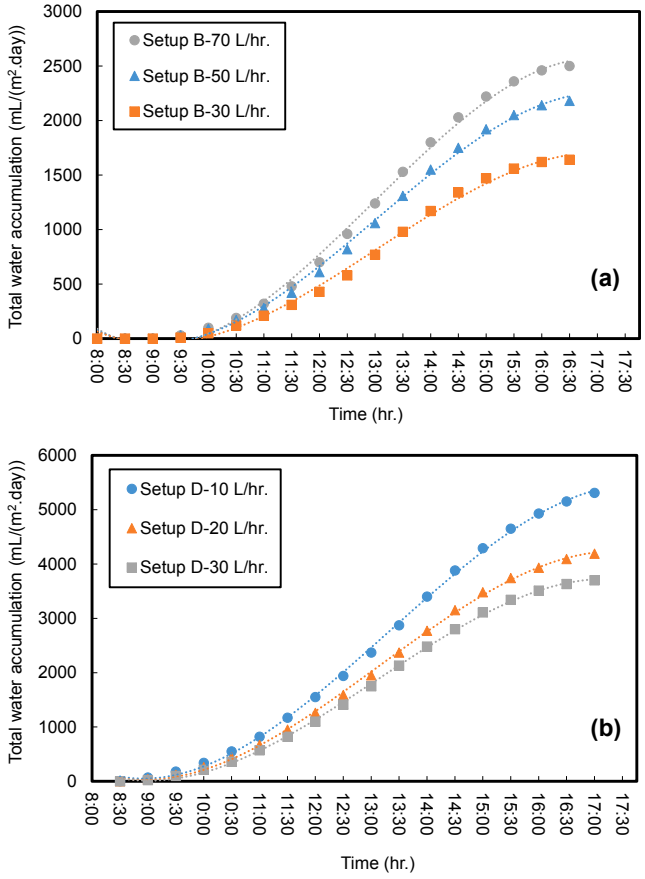

Fig. 6. Variation of daily total fresh-water accumulation versus local time for (a) setup B and (b) setup D.

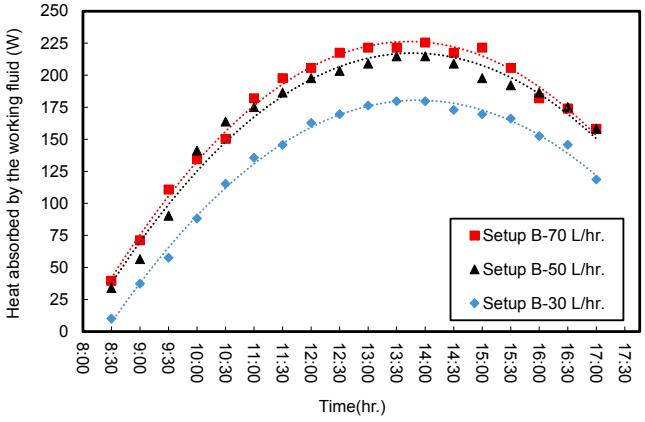

Fig. 7. Variation of heat absorbed by the working fluid versus time for setup B.

Fig. 7 displays the variation of heat absorbed by the working fluid versus time for setup B with flow rates of 30 L/hr, 50 L/hr, and 70 L/hr. From Fig. 7 it is clearly seen that by increasing the flow rate from 30 L/hr to 50 L/h, the heat absorbed by the working fluid is improved by 24.53%. However, increasing the flow rate from 50 L/hr to 70L/h has a negligible effect on the improvement of this value. These results indicate that the 50 L/hr is appropriate by considering the pump power consumption (see Fig. 6(a)).

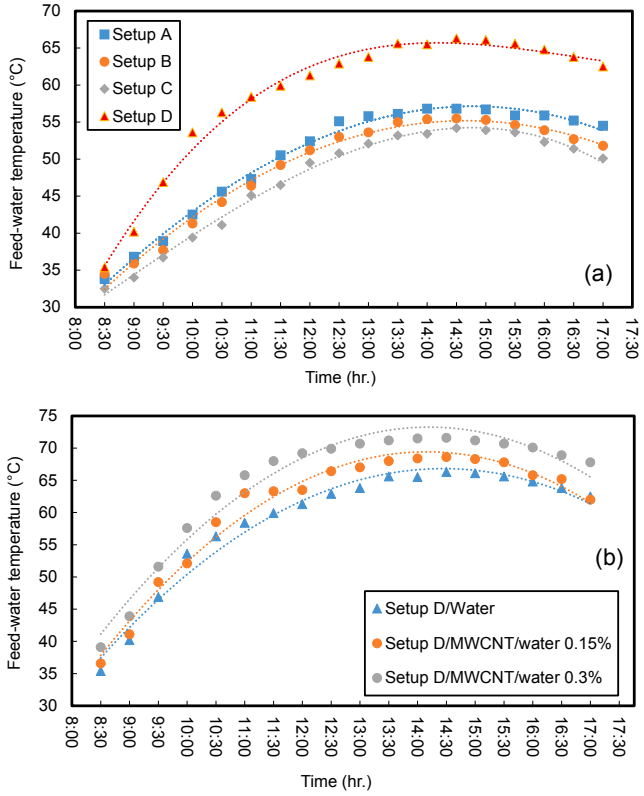

Fig. 8. Variation of feed-water temperature in (a) setup A-D and (b) setup D using different HTFs.

4.3. Analysis of feed-water temperature

As mentioned before, the feed-water temperature of all studied setups is measured during the experiments using a calibrated PT-100 thermocouple which is linked to a digital indicator. The variation of feed-water temperature for setup A-D is illustrated in Fig. 8(a). In addition, the variation of feed-water temperature for setup D employing deionized water and MWCNTs/water nanofluid with mass fractions of 0.15 and 0.3% as the HTF is shown in Fig. 8(b). It can be seen from Fig. 8(a) and (b) that, in all setups the maximum feed-water temperature is obtained during the period from 13 pm to 16 pm. Based on Fig. 8(a) the average feed-water temperature of setup A is 50.37 °C. Compared to setup A, by adding an internal condenser (setup B), the average feed-water temperature is reduced to 48.95 °C. When three thermoelectric coolers are also added to the system (setup C), the average feed-water temperature is 47.21 °C. However, as compared to setups B and C, when a heat exchanger connected to the STS is added to the system (setup D), the feed-water temperature is increased by 9.87 and 11.61 °C, respectively. As shown in Fig. 8(b), by replacing the MWCNTs/water nanofluid with mass fractions of 0.15 and 0.3% instead of water, the average feed-water temperature will be increased by 2.23 °C and 5.69 °C, respectively. In fact, better thermal properties of nanofluid compared to water lead to more heat transfer rates between the HTF and feed-water, and a substantial effect on the performance and evaporation rate inside the solar still.

4.4. Fresh-water accumulation

As discussed in the previous sections, the selected flow rates for the condenser working fluid and the HTF are 50 L/hr and 10 L/hr, respectively. In this section, all studied setups are compared in terms of daily, nightly, and total fresh-water accumulation during the experiments. The variation of the hourly and daily fresh-water accumulation

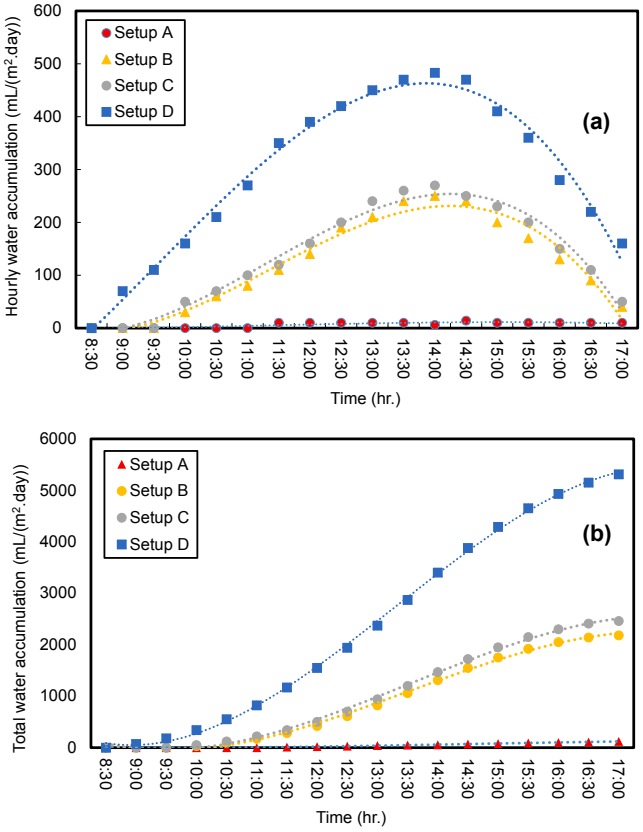

Fig. 9. Variation of (a) hourly and (b) daily total fresh-water accumulation versus local time for setup A-D using water as HTF.

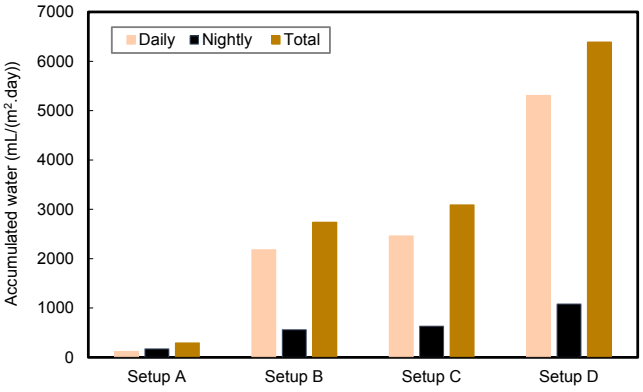

Fig. 10. Daily, nightly, and total yield of fresh-water for setups A-D using water as HTF.

versus local time during the tests (8:00–17:00) for setup A-D are illustrated in Fig. 9(a) and (b), respectively. Moreover, Fig. 10 shows the daily (8:00–17:00), nightly (17:00–8:00) and total fresh-water accumulation (summation of daily total and nightly) for the four setups. Based on Fig. 9(a) and (b), it is clear that, although the feed-water temperature of setup A is higher than that of setups B and C, the hourly and daily total fresh-water of setup A is too low. This is because setup A does not include any cold surfaces as a condenser. It should be noted that both evaporation and condensation are important issues for fresh-water production. Increasing feed-water temperature without having a condensing surface has a negligible effect on CSS efficiency. Fig. 8(a) shows that trends of hourly fresh-water for setups B and C are approximately the same and the maximum rate happens at 13:30–14:30. However, the fresh-water of setup D is markedly enhanced by increasing the feed-water temperature with the aid of a heat exchanger

and Fresnel lenses. To increase the efficiency of the CSS, by adding an internal condenser with an inlet working fluid temperature of 20 °C (setup B) and three external thermoelectric coolers (setup C), the daily total fresh-water is enhanced nearly by 1716.67% and 1950%, respectively, compared to that of the CSS. The reason for the considerable improvement in fresh-water production is adding a condenser to the system in setups B and C. In order to increase the feed-water temperature of the CSS, setup D has a spiral heat exchanger linked to the STS with three linear Fresnel lenses as a concentrator. Due to a higher feed-water temperature and the existence of condenser, the amount of total fresh-water production of setup D is more than setups A-C. The amount of fresh-water produced up to 17o'clock for setup B, C, and D is 2180, 2460, and 5310 mL, respectively.

Atmosphere with a lower temperature at night (17:00–8:00) results in the release of the stored thermal energy and production of more fresh-water. According to Fig. 10, the amount of fresh-water produced in the night period is significantly lower than the amount produced during the day. This is because only the remaining water vapor in the system is condensed at night. As the amount of remaining vapor for setup B and C in nearly the same, the amount of nocturnal water for these setups are almost the same. For setup D which is equipped with the STS, the remaining vapor at the end of the day is significantly more, therefore, the nocturnal water production in this setup is more than that of the other setups. The nightly fresh-water produced in setup D is 910 mL more than that of setup A, 520 mL more than that of setup B, and 450 mL more than that of setup C. The results from Fig. 10 shows the total yield of fresh-water of setup D is 133.21% and 106.98% more than setups B and C, respectively.

4.5. Effects of the fluid type of HTF in setup D

Based on work by Muraleedharan et al. [31], using a nanofluid as HTF has an inevitable effect on fresh-water production of the CSS; therefore, in this section, the effects of various HTFs (deionized water, and MWCNTs/water) are investigated on the fresh-water production. Fig. 11(a) displays the variation of daily total fresh-water accumulation versus local time for setup D for various HTFs. Moreover, Fig. 11(b) shows the daily, nightly, and total yield (summation of daily and nightly) of fresh-water for setup D. The results in Fig. 11(a) shows that using of MWCNTs/water with mass fractions of 0.3 and 0.15% instead of deionized water can increase daily total fresh-water production by 31.6% and 11.84%, respectively. The reason for the fresh-water increase maybe because of the better thermal conductivity of the MWCNTs/water nanofluid in comparison with the deionized water. It means that the rate of absorbing heat from the collector and releasing heat to the feed-water in MWCNTs/water nanofluid is more than deionized water. Regarding the results presented in Fig. 11(b), it could be concluded that by summation of the daily and nightly fresh-water, the total yield for setup D is 6390 mL/(m^2·day), 6990 mL/(m^2·day), and 8150 mL/(m^2·day) in the case of deionized water, MWCNTs/water 0.15%, and MWCNTs/water 0.3%, respectively. In addition, the values of nightly fresh-water prove that the feed-water temperature at the end of the day in the cases of nanofluid, as the HTF, is more than deionized-water which in turn leads to an increase of the fresh water production at night. Adding nanoparticles in the base-fluid can increase the heat transfer rate and thereby enhancing the feed-water evaporation rate. As stated earlier, the main purpose of the current study is to enhance the performance of a CSS by employing a dual-axis solar tracking system. Thus, studying the effects of other mass fractions or other types of nanofluids is intended for future studies.

5. Energy analysis of different solar stills

In order to scrutinize the performance of considered solar stills, hourly and daily efficiencies should be calculated. In this section, based on the obtained experimental data, the system performance is studied.

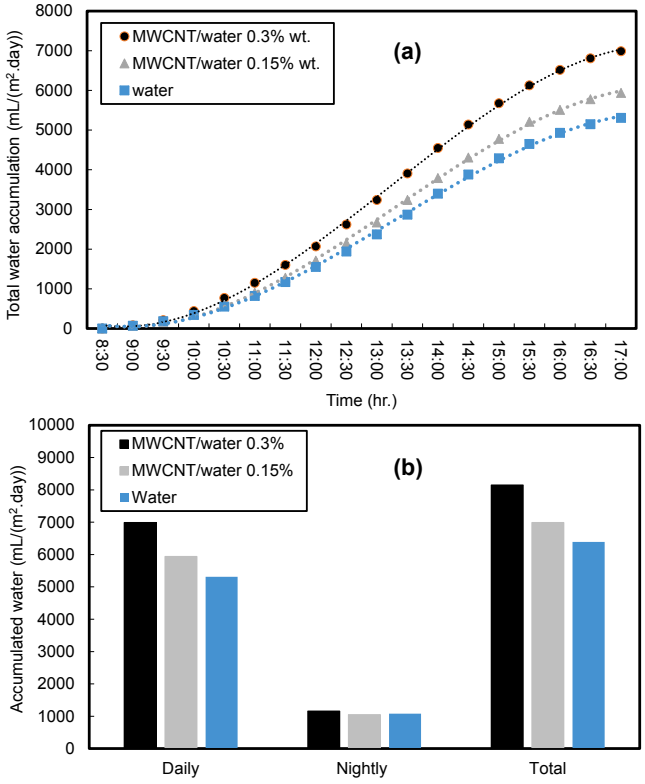

Fig. 11. Effect of different HTFs on (a) variation of daily total water accumulation versus local time of setup D and (b) daily, nightly, and total yield of fresh-water of setup D.

The hourly efficiencies in cases of CSS and CSS linked to STS could be determined based on the following two equations, respectively:

$$\eta_h = \frac{m \times h_{fg}}{A \times I(t) \times \Delta t} \times 100 \quad (1)$$

$$\eta_h = \frac{m \times h_{fg}}{A \times I(t) \times \Delta t + \dot{m} \times c \times \Delta t} \times 100 \quad (2)$$

Here, m and h_{fg} are fresh-water distilled mass (kg) and the latent heat of feed-water (J/kg). Moreover, A and $I(t)$ represent basin area (m^2) and the received average solar irradiation. In Eq. (2), the term ($\dot{m} \times c \times \Delta t$) is the thermal energy provided by the STS in which, $\dot{m}$, c, and Δt are the HTF mass flow rate (kg/s), HTF specific heat capacity (J/kg.K), and the difference between inlet/outlet temperatures (°C) in the STS. The Daily average efficiency of considered solar stills is defined as:

$$\eta_D = \frac{\sum \eta_h}{n} \quad (3)$$

Here, η_h and n are hourly efficiency and total working hours, respectively.

Fig. 12 shows the daily average efficiency of considered solar stills. From Fig. 9, it is found that due to increasing fresh-water production, setups B and C elevate the daily average efficiency. For instance, the daily average efficiencies obtained by Eq. (3) for setup A, B, and C are 1.48, 19.66, and 22.87%, respectively. Furthermore, it is found that the solar stills linked to the STS with MWCNT/water nanofluid 3% wt. gives the best result. In fact, MWCNTs nanoparticles due to their high thermal properties and their Brownian motion, particle migration and other unique heat transfer mechanisms in the pure base fluid (water) lead to enhancing system efficiency. For instance, by using the nanofluid with a mass fraction of 0.15 and 0.3%, the daily average efficiency is increased about 9.56 and 17.85%, respectively, compared to pure water.

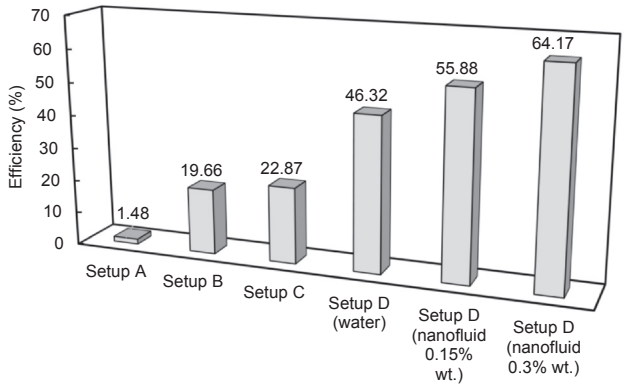

Fig. 12. The average efficiency of considered setups.

6. Cost analysis of different solar stills

A cost analysis is carried out based on the presented method in Refs. [35,36] for three experimental setups considered in this paper. The total annual cost (*TAC*) for 1 L fresh-water production encompasses various parameters as:

$$TAC = AFC + AMC - ASV \tag{4}$$

in which, the *AFC* is annual first cost, *AMC* annual maintenance cost, and *ASC* annual salvage cost. The annual first cost can be stated as:

$$AFC = CRF \times \text{Initial investment} \tag{5}$$

in which, the CRF is the capital recovery factor calculated using:

$$CRF = \frac{i \times (i+1)^n}{(i+1)^n - 1} \tag{6}$$

where n is the prospect period for the system (10 years) and i is the annual interest rate (20%). Based on Eq. (4), the AMC and system salvage value (S) is considered 30% of AFC and 10 % of the initial cost:

$$ASV = S \times SFF \tag{7}$$

In the above equation, the *SFF* is the sinking fund factor calculated as:

$$\text{SFF} = \frac{\text{i}}{(\text{i}+1)^{\text{n}} - 1} \tag{8}$$

By considering *Q* as the total volume of fresh-water produced, it can be considered that the cost of 1 L of distilled water is:

$$1\ \text{L} = \frac{\text{AFC}}{\text{Q}} \tag{9}$$

On the basis of outdoor experimental results, the fresh-water production of setups A, C, $D_{(water)}$, and $D_{(nanofluid)}$ are 0.29 L/day, 3.09 L/day, 6.39 L/day, and 8.15 L/day, respectively. Regarding Mashhad weather conditions, it is assumed that the considered solar stills run 320 days during the year (sunny and stable days). Therefore, the cost of fresh-water production from setup A, C, D (water), and D (nanofluid) is obtained as 0.24, 0.31, 0.039 and 0.034 $/liter, respectively. In Table 4, a comparison is given based on the above-mentioned results for different considered setups.

Table 4
A summary of cost analysis on considered setups.

Setup	HTF	Lifetime (year)	TAC for period ($)	Total fresh water produced (L)	The cost of 1L ($)
Setup A	–	10	227.70	928	0.24
Setup C	–	10	310.28	9888	0.031
Setup D	Water	10	813.12	20448	0.039
Setup D	MWCNTs/water (0.3 wt. %)	10	903.54	26080	0.034

6.1. Results comparison

As stated previously, the focus of this study is on the effects of water and MWCNTs/water nanofluid as the HTFs on the performance of CSS equipped with a dual-axis STS and linear Fresnel lens. Different designs of solar stills have been investigated by various research groups in the literature and their results are compared with those of the present study in Table 5. The results for fresh-water yield, overall efficiency, and cost per liter of distilled water are provided in this table. The available experiments in the literature on CSS equipped with a dual-axis STS to enhance the performance are limited. It is clearly observed that the accumulated fresh-water yield values are low ($\leq$5 kg/m^2·day) in the works of Agrawal and Rana [37], Ketabchi et al. [38], Al-harahsheh et al. [39], Yousef and Hassan [40], Vigneswaran [41], and Rajaseenivasan and Murugavel [42]. Moreover, it is found that the solar stills by Rajesh et al. [43], Morad et al. [44] and Hassan [45] have low efficiency ($\leq$30%). As shown in Table 5, although the proposed solar still designs by Wu et al. [46] lead to a suitable value for accumulated fresh-water yield during a day, their results are not analyzed from the efficiency/cost viewpoints. The fresh-water productivity and efficiency of the present study (nanofluid-based solar still with STS) are higher than those given in Refs. [47,48].

7. Conclusion

In this research, the idea of connecting the CSS to STS equipped with Fresnel lenses was experimentally investigated. Four various setups including; the CSS; the CSS with an internal condenser; the CSS with an internal condenser and external thermoelectric coolers; and the CSS with a dual-axis STS equipped with Fresnel lenses were designed and fabricated. A series of experiments were first performed to select appropriate flow rates of condenser working fluid and HTF. Next, the effects of deionized water, MWCNTs/water nanofluid with two mass fractions of 0.15 and 0.3% as the HTF were studied on fresh-water productivity. The results of four setups in various operating conditions were compared to each other. The entire experiments were executed on non-cloudy and stable days of June 2019.

Based on this study, the following conclusions are made:

- From a series of experiments, the condenser working fluid and HTF flow rates were selected as 50 L/hr and 10 L/hr, respectively.
- Increasing feed-water temperature without adding a condenser had a negligible effect on fresh-water productivity.
- Adding an internal condenser and simultaneous internal condenser and thermoelectric coolers as condenser surface enhanced total fresh-water production approximately by 844 and 965%, respectively, compared to that of the CSS.
- The daily, nightly, and total yield of fresh-water presented solar still (the CSS with STS) with deionized water as HTF compared to that of the CSS was increased by 5190, 910, and 6100 mL/(m^2·day), respectively.
- For the CSS with the STS system, using MWCNTs/water nanofluid 0.15 and 0.3% wt. enhanced the total fresh-water productivity by 9.38% and 27.54%, respectively, compared to that of the deionized water.
- The cost of fresh-water production from setup A, C, D (water), and D (nanofluid) was obtained as 0.24, 0.31, 0.039 and 0.034 $/liter, respectively.
- By increasing the nanofluid mass fraction from 0.15% to 0.3%, the daily average efficiency was increased about 9.56 and 17.85%, respectively, compared to pure water.

Table 5
Comparison of available experimental results in the literature with those of the present study in terms of design, accumulated yield, overall efficiency, and cost.

Author(s)	Design of experimental setup	Accumulated yield (kg/(m^2.day)	Overall efficiency (%)	Cost per liter of distilled water
Wu et al. [46]	Effect of linear Fresnel lens on solar still performance	15.16	N/A	N/A
Rajesh VR et al. [43]	Solar still equipped with a spot Fresnel lens	7	24	N/A
Al-harahsheh et al. [39]	Solar still equipped with external solar collector	4.3	N/A	0.05
Morad et al. [44]	Solar still equipped with a solar collector	10.06	80.6	N/A
Kabeel and Abdelgaied [47]	Solar still utilizing paraffin wax as a thermal energy storage	7.54	N/A	0.03
Yousef and Hassan [40]	Solar still with porous media in the water basin	3.68	36.9	0.05
Rajaseenivasan and Murugavel. [49]	Effect of single and double basin slope on performance solar still	4.75	N/A	N/A
Nazari et al. [48]	Solar still coupled with thermoelectric cooler	5.63	N/A	0.0252
Muraleedharan et al. [31]	Effect of Al_2O_3/water nanofluid and linear Fresnel lens on the performance of a solar still	12.19	53.55	0.0197
Hassan [45]	Solar still equipped with a parabolic collector	8.53	22.96	0.0207
Ketabchi et al. [38]	Solar still linked to a external flat plate reflectors	4.2	36.7	N/A
Agrawal and Rana [37]	Conventional solar still	6.2	41.99	N/A
Vigneswaran et al. [41]	Solar still coupled with phase change material as a heat energy storage	4.4	46.29	N/A
Present study		8.15	64.17	0.034

Declaration of Competing Interest

The authors declare that they have no known competing financial interests or personal relationships that could have appeared to influence the work reported in this paper.

Acknowledgments

The Research of The Corresponding Author is supported by a Grant from the Ferdowsi University of Mashhad (1/49612).

References

[1] K. Sampathkumar, T.V. Arjunan, P. Pitchandi, P. Senthilkumar, Active solar distillation-A detailed review, Renew. Sustain. Energy Rev. 14 (2010) 1503–1526, https://doi.org/10.1016/j.rser.2010.01.023.
[2] X. Yang, L. Yan, F. Ran, Y. Huang, D. Pan, Y. Bai, et al., Graphical abstract, J. Memb. Sci. (2020), https://doi.org/10.1016/j.memsci.2019.117753.
[3] L. Yan, X. Yang, J. Long, X. Cheng, D. Pan, Y. Huang, et al., Strategy to construct water-unidirectional, Janus (2020) 478–481, https://doi.org/10.1039/c9cc08088k.
[4] D. Guo, Y. Xiao, T. Li, Q. Zhou, L. Shen, R. Li, Fabrication of high-performance composite nanofiltration membranes for dye wastewater treatment: mussel-inspired, J. Colloid Interface Sci. (2019), https://doi.org/10.1016/j.jcis.2019.10.078.
[5] C. Charcosset, A review of membrane processes and renewable energies for desalination, Desalination 245 (2009) 214–231, https://doi.org/10.1016/j.desal.2008.06.020.
[6] D.B. Singh, J.K. Yadav, V.K. Dwivedi, S. Kumar, G.N. Tiwari, I.M. Al-Helal, Experimental studies of active solar still integrated with two hybrid PVT collectors, Sol. Energy 130 (2016) 207–223, https://doi.org/10.1016/j.solener.2016.02.024.
[7] M.E. Demir, I. Dincer, Development of an integrated hybrid solar thermal power system with thermoelectric generator for desalination and power production, Desalination 404 (2017) 59–71, https://doi.org/10.1016/j.desal.2016.10.016.
[8] Z.M. Omara, A.E. Kabeel, A.S. Abdullah, A review of solar still performance with reflectors, Renew. Sustain. Energy Rev. 68 (2017) 638–649, https://doi.org/10.1016/j.rser.2016.10.031.
[9] A. Muthu Manokar, D. Prince Winston, A.E. Kabeel, S.A. El-Agouz, R. Sathyamurthy, T. Arunkumar, et al., Integrated PV/T solar still- A mini-review, Desalination 435 (2018) 259–267, https://doi.org/10.1016/j.desal.2017.04.022.
[10] M.C. Yadav, Water desalination system using solar heat: A review, Renew. Sustain. Energy Rev. 67 (2017) 1308–1330, https://doi.org/10.1016/j.rser.2016.08.058.
[11] H. Sharon, K.S. Reddy, A review of solar energy driven desalination technologies, Renew. Sustain. Energy Rev. 41 (2015) 1080–1118, https://doi.org/10.1016/j.rser.2014.09.002.
[12] G.N. Tiwari, H.N. Singh, R. Tripathi, Present status of solar distillation, Sol. Energy 75 (2003) 367–373, https://doi.org/10.1016/j.solener.2003.07.005.
[13] F.F. Tabrizi, M. Dashtban, H. Moghaddam, K. Razzaghi, Effect of water flow rate on internal heat and mass transfer and daily productivity of a weir-type cascade solar still, Desalination 260 (2010) 239–247, https://doi.org/10.1016/j.desal.2010.03.037.
[14] D.B. Singh, Improving the performance of single slope solar still by including N identical PVT collectors, Appl. Therm. Eng. 131 (2018) 167–179, https://doi.org/10.1016/j.applthermaleng.2017.11.146.
[15] A.K. Tiwari, G.N. Tiwari, Effect of water depths on heat and mass transfer in a passive solar still: in summer climatic condition, Desalination 195 (2006) 78–94, https://doi.org/10.1016/j.desal.2005.11.014.
[16] M. Edalatpour, K. Aryana, A. Kianifar, G.N. Tiwari, O. Mahian, S. Wongwises, Solar stills: A review of the latest developments in numerical simulations, Sol. Energy 135 (2016) 897–922, https://doi.org/10.1016/j.solener.2016.03.005.
[17] H. Tanaka, Y. Nakatake, One step azimuth tracking tilted-wick solar still with a vertical flat plate reflector, Desalination 235 (2009) 1–8, https://doi.org/10.1016/j.desal.2008.01.011.
[18] S. Suman, M. Kaleem, M. Pathak, Performance enhancement of solar collectors—A review, Renew. Sustain. Energy Rev. 49 (2015) 192–210, https://doi.org/10.1016/j.rser.2015.04.087.
[19] F. Dähler, M. Wild, R. Schäppi, P. Haueter, T. Cooper, Optical design and experimental characterization of a solar concentrating dish system for fuel production via thermochemical redox cycles, Sol. Energy 170 (2018) 568–575, https://doi.org/10.1016/j.solener.2018.05.085.
[20] B. Chaouchi, A. Zrelli, S. Gabsi, Desalination of brackish water by means of a parabolic solar concentrator, Desalination 217 (2007) 118–126, https://doi.org/10.1016/j.desal.2007.02.009.
[21] S. Kumar, A. Tiwari, Design, fabrication and performance of a hybrid photovoltaic/thermal (PV/T) active solar still, Energy Convers. Manag. 51 (2010) 1219–1229, https://doi.org/10.1016/j.enconman.2009.12.033.
[22] F. Saeedi, F. Sarhaddi, A. Behzadmehr, Optimization of a PV/T (photovoltaic/thermal) active solar still, Energy 87 (2015) 142–152, https://doi.org/10.1016/j.energy.2015.04.062.
[23] P. Hooshmand, M.B. Shafii, R. Roshandel, An experimental study of a solar hybrid system to produce freshwater from waste heat of photovoltaic module by using thermosyphon heat pipes, Energy Convers. Manag. 158 (2018) 9–22, https://doi.org/10.1016/j.enconman.2017.12.043.
[24] A. Hosseini, A. Banakar, S. Gorjian, Development and performance evaluation of an active solar distillation system integrated with a vacuum-type heat exchanger, Desalination (2017) 1–15, https://doi.org/10.1016/j.desal.2017.12.031.
[25] M. Imtiaz Hussain, A. Ali, G.H. Lee, Performance and economic analyses of linear and spot Fresnel lens solar collectors used for greenhouse heating in South Korea, Energy 90 (2015) 1522–1531, https://doi.org/10.1016/j.energy.2015.06.115.
[26] A. Banakar, S. Saghar, A. Motevali, G. Najafi, Evaluation of a pre-heating system for solar desalination system with linear Fresnel lens, J. Renew. Sustain. Energy 9 (2017), https://doi.org/10.1063/1.5006206.
[27] V. Kumar, R.L. Shrivastava, S.P. Untawale, Fresnel lens: A promising alternative of reflectors in concentrated solar power, Renew. Sustain. Energy Rev. 44 (2015) 376–390, https://doi.org/10.1016/j.rser.2014.12.006.
[28] Y. Qiu, Y.L. He, M. Wu, Z.J. Zheng, A comprehensive model for optical and thermal characterization of a linear Fresnel solar reflector with a trapezoidal cavity receiver, Renew. Energy 97 (2016) 129–144, https://doi.org/10.1016/j.renene.2016.05.065.
[29] S.I. Palomino-Resendiz, D.A. Flores-Hernández, N. Lozada-Castillo, L. Guzmán-Vargas, A. Luviano-Juárez, Design and implementation of a robotic active solar distiller based on a Fresnel concentrator and a photovoltaic system, Energy Convers. Manag. 166 (2018) 637–647, https://doi.org/10.1016/j.enconman.2018.04.069.
[30] R. Sathyamurthy, S.A. El-Agouz, P.K. Nagarajan, J. Subramani, T. Arunkumar, D. Mageshbabu, et al., A review of integrating solar collectors to solar still, Renew. Sustain. Energy Rev. 77 (2017) 1069–1097, https://doi.org/10.1016/j.rser.2016.11.223.
[31] M. Muraleedharan, H. Singh, M. Udayakumar, S. Suresh, Modified active solar distillation system employing directly absorbing Therminol 55–Al2O3 nano heat transfer fluid and Fresnel lens concentrator, Desalination 457 (2019) 32–38, https://doi.org/10.1016/j.desal.2019.01.024.

[32] A. Taheri, M. Ghasemian, M. Mohammadi, A new design of liquid-cooled heat sink by altering the heat sink heat pipe application: Experimental approach and prediction via artificial neural network, Energy Convers. Manag. 206 (2020) 112485, https://doi.org/10.1016/j.enconman.2020.112485.
[33] M. Sardarabadi, M. Passandideh-fard, S. Zeinali, Experimental investigation of the effects of silica/water nanofluid on PV/T (photovoltaic thermal units), Energy 66 (2014) 264–272, https://doi.org/10.1016/j.energy.2014.01.102.
[34] A. Kazemian, M. Hosseinzadeh, M. Sardarabadi, M. Passandideh-Fard, Experimental study of using both ethylene glycol and phase change material as coolant in photovoltaic thermal systems (PVT) from energy, exergy and entropy generation viewpoints, Energy 162 (2018) 210–223, https://doi.org/10.1016/J.ENERGY.2018.07.069.
[35] K.R. Ranjan, S.C. Kaushik, H. Khas, T. Education, N. Delhi, Economic feasibility evaluation of solar distillation systems based on the equivalent cost of environmental degradation and high-grade energy savings, Int. J. Low-Carbon Technol. (2013) 1–8, https://doi.org/10.1093/ijlct/ctt048.
[36] K. Mukherjee, G.N. Tiwari, Economic analyses of various designs of conventional solar stills, Energy Convers. Manage. 26 (1986) 155–157.
[37] A. Agrawal, R.S. Rana, Theoretical and experimental performance evaluation of single-slope single-basin solar still with multiple V-shaped floating wicks, Heliyon (2019), https://doi.org/10.1016/j.heliyon.2019.e01525.
[38] F. Ketabchi, S. Gorjian, S. Sabzehparvar, Z. Shadram, Experimental performance evaluation of a modified solar still integrated with a cooling system and external flat-plate reflectors, Sol. Energy 187 (2019) 137–146, https://doi.org/10.1016/j.solener.2019.05.032.
[39] M. Al-harahsheh, M. Abu-arabi, H. Mousa, Z. Alzghoul, Solar desalination using solar still enhanced by external solar collector and PCM, Appl. Therm. Eng. 128 (2018) 1030–1040, https://doi.org/10.1016/j.applthermaleng.2017.09.073.
[40] M.S. Yousef, H. Hassan, Assessment of different passive solar stills via exergoeconomic, exergoenvironmental, and exergoenviroeconomic approaches: A comparative study, Sol. Energy 182 (2019) 316–331, https://doi.org/10.1016/j.solener.2019.02.042.
[41] V.S. Vigneswaran, G. Kumaresan, B.V. Dinakar, K.K. Kamal, R. Velraj, Augmenting the productivity of solar still using multiple PCMs as heat energy storage, J. Energy Storage 26 (2019) 101019, https://doi.org/10.1016/j.est.2019.101019.
[42] K. Srithar, T. Rajaseenivasan, Recent fresh water augmentation techniques in solar still and HDH desalination – A review, Renew. Sustain. Energy Rev. 82 (2018) 629–644, https://doi.org/10.1016/j.rser.2017.09.056.
[43] V.R. Rajesh, K. Harikrishnan, K.K. Chaithanya, S. Salim, Performance evaluation of a solar desalination system integrated with a Fresnel lens concentrator, Int. J. Renew. Energy Res. 6 (2016).
[44] M.M. Morad, H.A.M. El-maghawry, K.I. Wasfy, Improving the double slope solar still performance by using flat-plate solar collector and cooling glass cover, DES 373 (2015) 1–9, https://doi.org/10.1016/j.desal.2015.06.017.
[45] H. Hassan, Comparing the performance of passive and active double and single slope solar stills incorporated with parabolic trough collector via energy, exergy and productivity, Renew. Energy (2019), https://doi.org/10.1016/j.renene.2019.10.050.
[46] G. Wu, H. Zheng, X. Ma, C. Kutlu, Y. Su, Experimental investigation of a multi-stage humidification-dehumidification desalination system heated directly by a cylindrical Fresnel lens solar concentrator, Energy Convers. Manag. 143 (2017) 241–251, https://doi.org/10.1016/j.enconman.2017.04.011.
[47] A.E. Kabeel, M. Abdelgaied, Improving the performance of solar still by using PCM as a thermal storage medium under Egyptian conditions, DES 383 (2016) 22–28, https://doi.org/10.1016/j.desal.2016.01.006.
[48] S. Nazari, H. Safarzadeh, M. Bahiraei, Performance improvement of a single slope solar still by employing thermoelectric cooling channel and copper oxide nanofluid: An experimental study, J. Clean. Prod. (2018), https://doi.org/10.1016/j.jclepro.2018.10.194.
[49] T. Rajaseenivasan, K.K. Murugavel, Theoretical and experimental investigation on double basin double slope solar still, DES 319 (2013) 25–32, https://doi.org/10.1016/j.desal.2013.03.029.